

# The Use of Technetium-99m for Intravital Tracing of Transplanted Multipotent Stromal Cells

D. N. Silachev<sup>1,2</sup>, A. K. Kondakov<sup>3,4</sup>, I. A. Znamenskii<sup>3,4</sup>, Yu. B. Kurashvili<sup>5,6</sup>,  
A. V. Abolenskaya<sup>6</sup>, N. R. Antipkin<sup>6</sup>, T. I. Danilina<sup>2</sup>, V. N. Manskikh<sup>2</sup>,  
M. V. Gulyaev<sup>7</sup>, Yu. A. Pirogov<sup>7</sup>, E. Yu. Plotnikov<sup>1,2</sup>, D. B. Zorov<sup>1,2</sup>,  
and G. T. Sukhikh<sup>1</sup>

Translated from *Kletochnye Tekhnologii v Biologii i Meditsine*, No. 3, pp. 188-195, July, 2016  
Original article submitted March 29, 2016

We studied the possibility of *in vivo* tracing of multipotent mesenchymal stromal cells labeled with a radiopharmaceutical preparation based on metastable isotope Technetium-99m and injected to rats with modeled traumatic brain injury. Accumulation of labeled cells occurred primarily in the liver and lungs. The cells distribution in internal organs greatly varied depending on the administration route. Cell injection into the carotid artery led to their significant accumulation in the damaged brain hemisphere, while intravenous injection was followed by diffuse cell distribution in all brain structures. Scintigraphy data were confirmed by magnetic resonance imaging and histological staining of cells. Visualization of stem cells labeled with Technetium-99m-based preparation by scintigraphy is an objective and highly informative method allowing real-time *in vivo* cell tracing in the body.

**Key Words:** *mesenchymal stem cells; scintigraphy; brain; imaging; tomography*

Active development of cell technologies and regenerative medicine requires techniques along tracing of transplanted stem cells in experimental and clinical studies. The kinetics of distribution of transplanted cells, their delivery to the target organs, and duration of their presence in different tissues remain beyond the scope of most studies. However, the kinetics of distribution of transplanted cells in the body is an essential characteristics for any cell product in both experimental and clinical studies, because it is an important criterion in assessing the efficiency of cell therapy.

In general, the efficiency of stem and progenitor cells in the therapy of various pathologies is beyond doubt [13]; however, the mechanisms underlying the positive effect of cell therapy are still debated. In this context, objective imaging of transplanted cells *in vivo* is essential for understanding of the pathways and rates of cell migration under normal and pathological conditions.

Until now, none of the proposed methods of detection of donor stem cells in the recipient body was accepted as a gold standard, which limits the use of cell technologies in clinical practice. The available imaging techniques are based on different principles of cell labeling and detection in the body and hence, these methods have different efficacy and limitations. Many methods proposed for experimental research on animals despite their high efficiency are not suitable for clinical trials. Eight parameters of an “ideal” stem cell marker for clinical trials were determined [9]: it should be biocompatible, safe for the patient, and nontoxic for cells; it should not induce genetic modi-

<sup>1</sup>V. I. Kulakov Research Center of Obstetrics, Gynecology, and Perinatology, Ministry of Health of the Russian Federation; <sup>2</sup>A. N. Belozersky Institute of Physico-Chemical Biology, M. V. Lomonosov Moscow State University; <sup>3</sup>N. I. Pirogov National Russian Research Medical University, Ministry of Health of the Russian Federation; <sup>4</sup>Hospital for Incurable Patients — Research Medical Rehabilitation Center; <sup>5</sup>National Research Nuclear University MEPhI; <sup>6</sup>P. A. Hertsen Moscow Oncology Research Institute; <sup>7</sup>Laboratory of Magnetic Tomography and Spectroscopy, Faculty of Fundamental Medicine, M. V. Lomonosov Moscow State University, Moscow, Russia. **Address for correspondence:** zorov@genebee.msu.ru. D. B. Zorov

fications in cells; it should allow cell quantitation in any anatomic location and detection of small amount of cells; it should not be diluted during cell division; transfer of this marker from labeled stem cell to tissues or body fluids should be minimum; it should allow detection by non-invasive imaging technologies over months; and it should not require additional injectable contrast agents for imaging. Although some markers possess some of these characteristics, none of them meets all the criteria.

Scintigraphy is a promising technique for detection of transplanted stem cells; and among radioactive labels used in medicine, metastable isotope technetium-99m ( $^{99m}\text{Tc}$ ) seems to be the closest to “ideal marker”.

Our aim was to develop a method of *in vivo* detection of multipotent mesenchymal stromal cells (MMSC) labeled with a radiopharmaceutical preparation (RP) based on  $^{99m}\text{Tc}$  in rats with modeled traumatic brain injury and to evaluate the distribution of cells administered via different routes.

## MATERIALS AND METHODS

**Animals.** The experiments were performed on random-bred rats weighing 300-350 g; the animals were kept under standard vivarium conditions with 12-h light/dark cycle at constant temperature ( $22\pm 2^\circ\text{C}$ ). The experiments were performed with strict adherence to EU Directive 2010/63/EEC on Protection of Vertebrate Animals Used for Experimental and Other Scientific Purposes.

**Modeling of traumatic brain injury.** Before the surgery, the rats were anesthetized with chloral hydrate (300 mg/kg, intravenously). The brain trauma was modeled by the method of graded open brain contusion as described elsewhere [8]. In brief, the animal was placed in a stereotaxis, the skin on the head was shaved and cut along the median line. A 5-mm hole was drilled in the skull above the left sensorimotor cortex (2.5 laterally and 1.5 mm caudally from the bregma) with a cutter. A cylindrical stricker was placed into the drilled hole 3-mm below the dura mater. The injury was inflicted by a weight (50 mg) falling from a height of 10 cm onto the stricker. During these manipulations, the body temperature was maintained at  $37\pm 0.5^\circ\text{C}$  with an infrared lamp.

**MMSC culturing.** Bone marrow MSC were isolated and characterized at V. I. Kulakov Research Center of Obstetrics, Gynecology, and Perinatology. The cells were washed out from the bone with DMEM containing 2 mm EDTA (anticoagulant) through a syringe and then centrifuged in Ficoll-urografin density gradient ( $\rho=1.077\text{ g/ml}$ ) for 30 min at 200g. The fraction containing mononuclear cells (interphase ring)

was collected, resuspended in the medium, and re-centrifuged at 150g for 5 min. The pellet was resuspended in complete nutrient medium DMEM/F-12 (1:1) supplemented with 10% fetal calf serum and 0.02% gentamicin and transferred to 25-cm<sup>2</sup> flasks (Corning). After MMSC adhesion to plastic, nonadherent cells were removed and the adherent culture was grown until confluence. The number of viable cells was counted by staining with trypan blue and propidium iodide; suspensions with cell viability  $>90\%$  were used for culturing.

**$^{99m}\text{Tc}$  labeling of MMSC.** RF was prepared immediately before cell labeling by adding 5 ml  $^{99m}\text{Tc}$ -sodium pertechnetate to a vial with hexamethyl propyleneamine oxime (HMPAO) lyophilisate (Taksim; Diamed) under aseptic conditions. This results in the formation of a  $^{99m}\text{Tc}$ -HMPAO complex. The  $^{99m}\text{Tc}$ -pertechnetate solution was prepared not later than 24 h after previous elution of  $^{99m}\text{Tc}$  generator and 20 min before preparing RF in accordance with the instructions of HMPAO manufacturer and existing recommendations [15,16]. Freshly prepared RP was used for cell labeling within 15 min.

RP quality was controlled by ascending thin layer chromatography in 99.5% ethyl acetate for 7 min [16] with modifications proposed by quality control kit manufacturer (Biodex LLC). The chromatogram was analyzed using a system for detection and analysis of radioactive compounds (Bioscan MS-2000F) and a NZ-138/A well counter (Gamma). The ratio of peak areas corresponding to lipophilic complex  $^{99m}\text{Tc}$ -HMPAO at the chromatogram front and water-soluble impurities was calculated.

In each experiment,  $5\times 10^6$  MMSC were incubated with  $^{99m}\text{Tc}$ -HMPAO ( $350\pm 50\text{ MBq}$ ) for 20 min. The cell suspension was centrifuged for 5 min at 150g, twice washed in saline, and resuspended in 1 ml saline before intravenous or intraarterial injection. Total activity of labeled cells before administration was  $53\pm 23\text{ MBq}$ . These conditions were chosen in preliminary *in vitro* experiments based on previously published data [1].

MMSC labeled with  $^{99m}\text{Tc}$ -HMPAO ( $1.5\times 10^6$  cells) were injected into the left jugular vein or internal carotid artery in 24 h after trauma as described previously [4].

**Cell labeling with iron oxide microparticles IOMP.** For labeling with IOMP, the cells were grown in flasks ( $10^5/\text{ml}$ ) in DMEM and commercial IOMP preparation (SiMAG, 0.75  $\mu\text{g}$ ; Chemicell) was added in a concentration of 1  $\mu\text{l/ml}$ . The cells were incubated with SiMAG for 24 h at  $37^\circ\text{C}$  and 5%  $\text{CO}_2$ . After incubation, the cells were washed with 3 portions of 0.9% NaCl (PanEco), dissociated with 0.25% trypsin-EDTA, centrifuged at 150g, adjusted to a required concentration, and used for injection to animals.

**MMSC detection by *in vivo* scintigraphy.** Immediately after MMSC injection, the animals were fixed to a plastic plate. The plate was positioned horizontally in the detector of an SPECT/CT imaging system (Infinia 4, Hawkeye General Electric). Two detectors were positioned in such a way that the whole animal body was covered. The images were acquired simultaneously in the direct anterior and direct posterior projections in a static mode, energy window of 135–145 keV, in 512×512-pixel matrix up to 500,000 pulses. The images were processed using Xeleris 2.1, GE software.

***In vivo* MMSC detection by scintigraphy.** Magnetic resonance imaging (MRI) was carried out on a 7 T BioSpec 70/30 tomograph at the Laboratory of Magnetic Tomography and Spectroscopy, Faculty of Fundamental Medicine, M. V. Lomonosov Moscow State University. This tomograph belongs to Biospectrometry Center of Shared Use of Scientific Equipment and is a unique scientific instrument. The study was performed under general anesthesia (300 mg/kg chloral hydrate, intraperitoneally) in 3 days after intraarterial injection of IOMP as described previously [12].

**Histological analysis of the brain.** For neurohistological studies, the experimental animals were anesthetized with chloral hydrate and perfused transcardially with 200 ml cold saline and then with 100 ml 4% formaldehyde in 0.1 M phosphate buffer. Paraffin sections were processed routinely and stained by the Perls method.

The data were processed statistically using Statistica 6.0 software (StatSoft). The significance of differences in radioactive tracer content in the brain hemispheres within the same time interval was assessed using Mann—Whitney  $U$  test and between time points

1 and 16 h using paired Wilcoxon's test ( $W$ ). The data were presented as the mean±error of the mean.

## RESULTS

**Control of tracer quality.** The efficiency of  $^{99m}\text{Tc}$ -HMPAO complex formation was assessed by ascending thin layer chromatography (Fig. 1, *a*). The mean RP labeling efficiency was 30% (27–33%). Measurement of water- and lipid-soluble fractions in a well counter showed similar results: the efficiency of  $^{99m}\text{Tc}$ -HMPAO complex formation was 30.5% (29–33%) in this case. After administration of RP to rats, the  $^{99m}\text{Tc}$ -HMPAO complex accumulated primarily in the liver, urinary bladder, and intestine (Fig. 1, *b*).

**MMSC distribution in rat body.** MMSC distribution on scintigrams was assessed visually and by semiquantitative methods by analyzing the areas corresponding to brain hemispheres, liver, lungs, and bladder.

During the first hour after intravenous MMSC transplantation, visual analysis showed accumulation of the radioactive label in the lung, kidney, and partially in the liver and bladder (Figs. 2, 3). At later terms (16 h), redistribution of the label was observed on scintigrams: a decrease in label content in the lungs with its simultaneous enhanced accumulation in the liver and intestine. In the brain, no significant differences in MMSC accumulation (signal intensity) were revealed between the damaged and intact hemisphere in 1 and 16 h after transplantation ( $p_U=0.17$ ). In 16 h after transplantation, the total label content in the brain also did not change significantly ( $p_W=0.11$ ). A different pattern of label distribution in the brain was observed after intraarterial injection of MMSC (Fig. 2). In 1 h after transplantation, significant accumulation

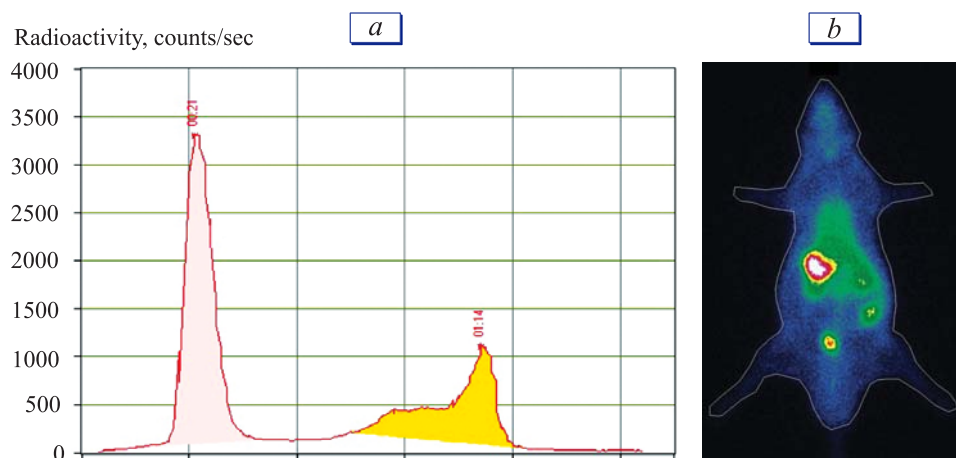


**Fig. 1.** Formation of  $^{99m}\text{Tc}$ -HMPAO complex and its distribution in the body. *a*) Representative chromatogram of the radioactivity distribution. Yellow peak corresponds to  $^{99m}\text{Tc}$ -HMPAO complex. Peak area reflects the effectiveness of complex formation. The content of water-soluble impurities is evaluated by the area of the pink peak. *b*) Planar scintigram in direct posterior projection 60 min after intravenous injection of  $^{99m}\text{Tc}$ -HMPAO complex.

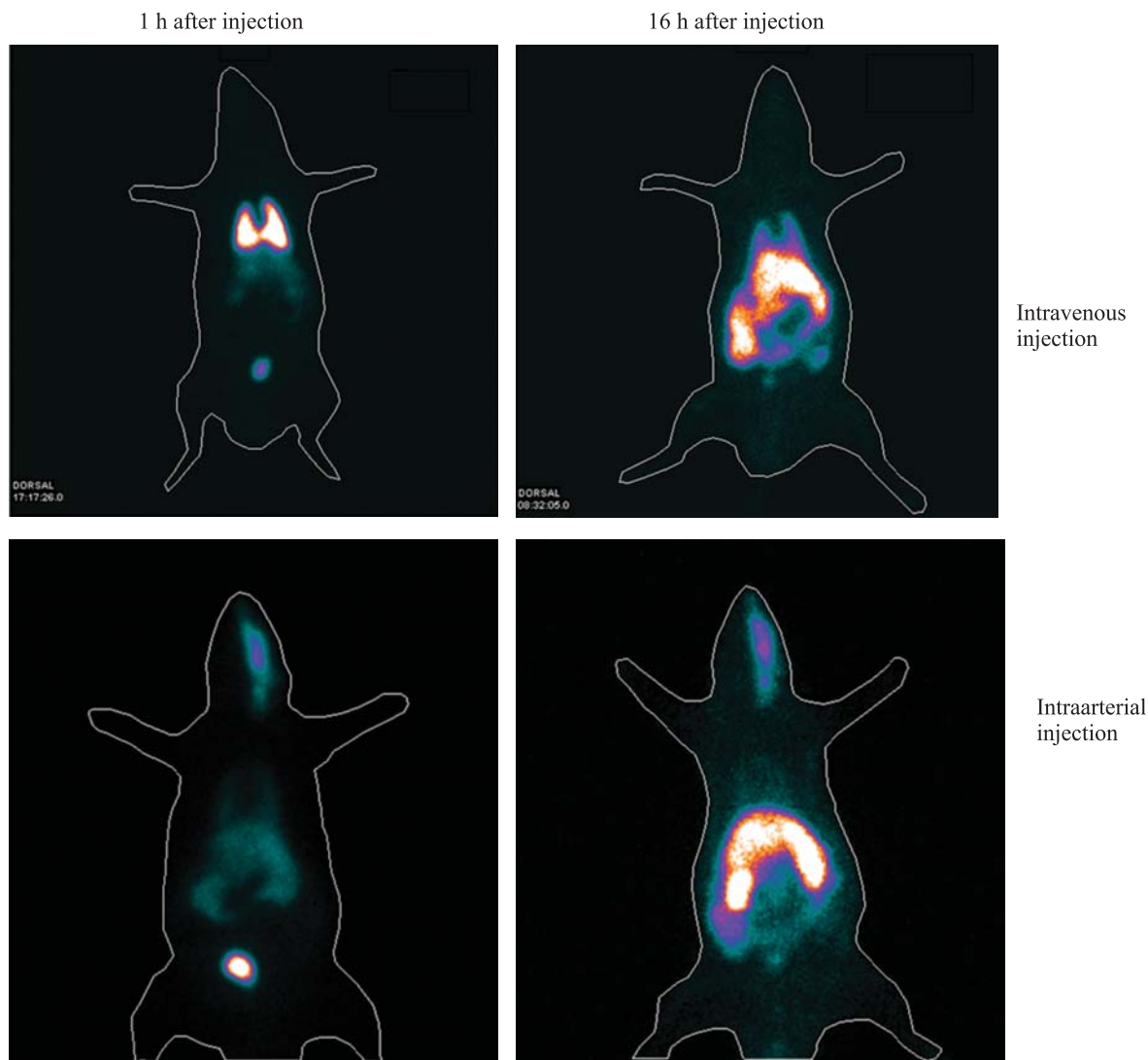


**Fig. 2.** MMSC distribution in rat body after intravenous and intraarterial injection. Planar scintigrams in direct posterior projection. All images are standardized by maximum accumulation.

of the label (19.6% of all injected label) was detected in the injured hemisphere on the side of injection, while label distribution in other organs was similar to that after intravenous administration. At later terms, redistribution of label towards the liver and kidneys was observed and by 16 h, the signal intensity in the injured hemisphere decreased to 10.5% of whole body activity (Fig. 3).

**MMSC distribution in the brain.** To check the correlation between label content in the brain and the presence of transplanted cells, we used an alternative method of MMSC visualization. The cells were labeled with IOMP, injected into the carotid artery, and then visualized by MRI in T2\*-weighed mode. Hypointensive (dark) signal in cells was detected within the hemisphere on the side of transplantation (Fig. 4). Labeled cells were diffusely distributed in all brain structures, including cortical and subcortical structures

(Fig. 4, *a, b*). For more precise location of MMSC in the brain tissue, histological examination was performed using special Perls staining for detection of iron particles. Analysis of histological preparations also confirmed the presence of MMSC in different parts of the brain; the cells demonstrating positive Perls staining were primarily detected in blood vessels or in the perivascular space (Fig. 4, *c, d*).

High therapeutic potential of stem cells is beyond doubt and their effectiveness and safety were confirmed in experimental studies on modeled pathologies and in clinical trials [13]. However, the mechanisms of the therapeutic effects of these cells remain an open question that cannot be answered without understanding of the kinetics of stem cell distribution in organs. Moreover, these studies should be carried out in humans, because animal experiments are insufficiently conclusive due to physiological and anatomical differ-

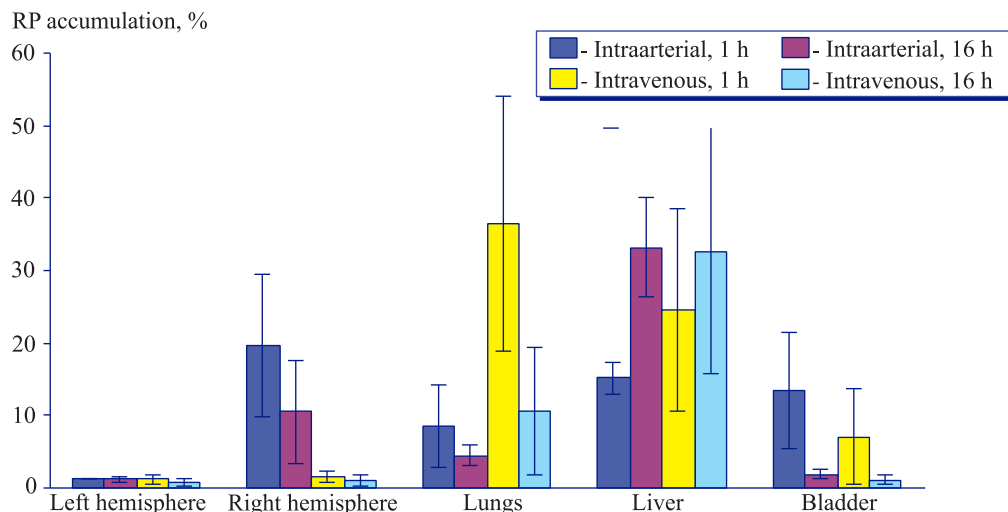


**Fig. 3.** Radioactivity distribution on rat organs relative to whole body radioactivity at different terms after injection and different administration routes.

ences. Various technologies were proposed for tracking stem cells in human tissues, including MRI and scintigraphy. However, MRI has serious limitations primarily because of long duration of whole body scanning protocols, and this method is useful only for imaging of the target organ. Scintigraphy seems to be more appropriate for evaluation of the distribution of transplanted stem cells labeled with a radioactive isotope in the body. Radioactive isotope  $^{99m}\text{Tc}$  is an available and most widely used in clinical practice. Its decay yields  $\gamma$ -radiation that possesses enough energy to pass all tissues and be recorded by a detector.  $^{99m}\text{Tc}$ -based preparations are long used in clinical practice for the diagnosis of distant metastases in the bone tissue, scintigraphy of the kidneys, thyroid gland, and other organs. The optimal time of visualization of RP distribution is determined by the radionuclide half-life. The half-life of  $^{99m}\text{Tc}$  is 6 h, which allows visualization  $^{99m}\text{Tc}$ -RP distribution within 24–30 h after injection. The time of visualization of RFP distribution also depends on the injected dose of radioactivity. We used clinical  $\gamma$ -chamber and traced the distribution of radiolabeled cells administered in a dose >50–70 MBq in 16 h after transplantation, though it proportionally increased the exposure for obtaining a single image.

$^{99m}\text{Tc}$ -HMPAO should be prepared with strict observation of certain rules. Only fresh eluate from continuously used generator should be used. The use of stabilizers, such as methylene blue, to prolong the life of RP is unacceptable when working with living cells, since these additives may reduce cell viability or affect their functional characteristics [5]. This as well as instability of the preparation dictate the need in RP quality control prior to use. The main radiochemical impurity of RFP is hydrophilic HMPAO complex that does not cross the cell membrane. The hydrophilic

and lipophilic components are separated by ascending thin-layer chromatography used by us.

When refining the procedure of preparing radioisotope label, we noted low labeling efficiency of the used RP, which can be due to variability of the chemical composition of either lyophilized HMPAO or eluate from the generator. Nevertheless, as secondary complexes do not cross cell membranes [11], they can be effectively removed by washing with saline or phosphate buffer, which ultimately allows attaining high efficiency of cell labeling.

One more limitation of using  $^{99m}\text{Tc}$ -HMPAO is instability of cell labeling. In particular, cell culture experiments showed that the rate of  $^{99m}\text{Tc}$ -HMPAO elimination from cells is  $\sim 7\%$  per hour [10], which can affect its distribution in the body and therefore lead to misinterpretation of the location of  $^{99m}\text{Tc}$ -HMPAO-labeled stem cells. In our study, these limitations did not significantly affect the accuracy of MMSC tracing at least within the observation time.

RP distribution in the body observed in our study generally agrees with previously described distribution in animals [2,6] and humans [1]. In most studies, the greater part of transplanted cells during the first hours is detected in the lungs. We also observed predominant accumulation of  $^{99m}\text{Tc}$ -HMPAO-labeled MMSC in the lungs. At the same time, the distribution was not static and changed considerably with time. The decrease of radioisotope signal in the lungs and its increase in the liver and kidneys with time are of particular importance. These findings indicate the need for thorough and sufficiently long tracing of transplanted cells for their detection in the target niches.

Comparison of RP distribution with circulation of free label seems to be also important. According a previous report [11],  $\sim 5\%$  label ( $^{99m}\text{Tc}$ -HMPAO)

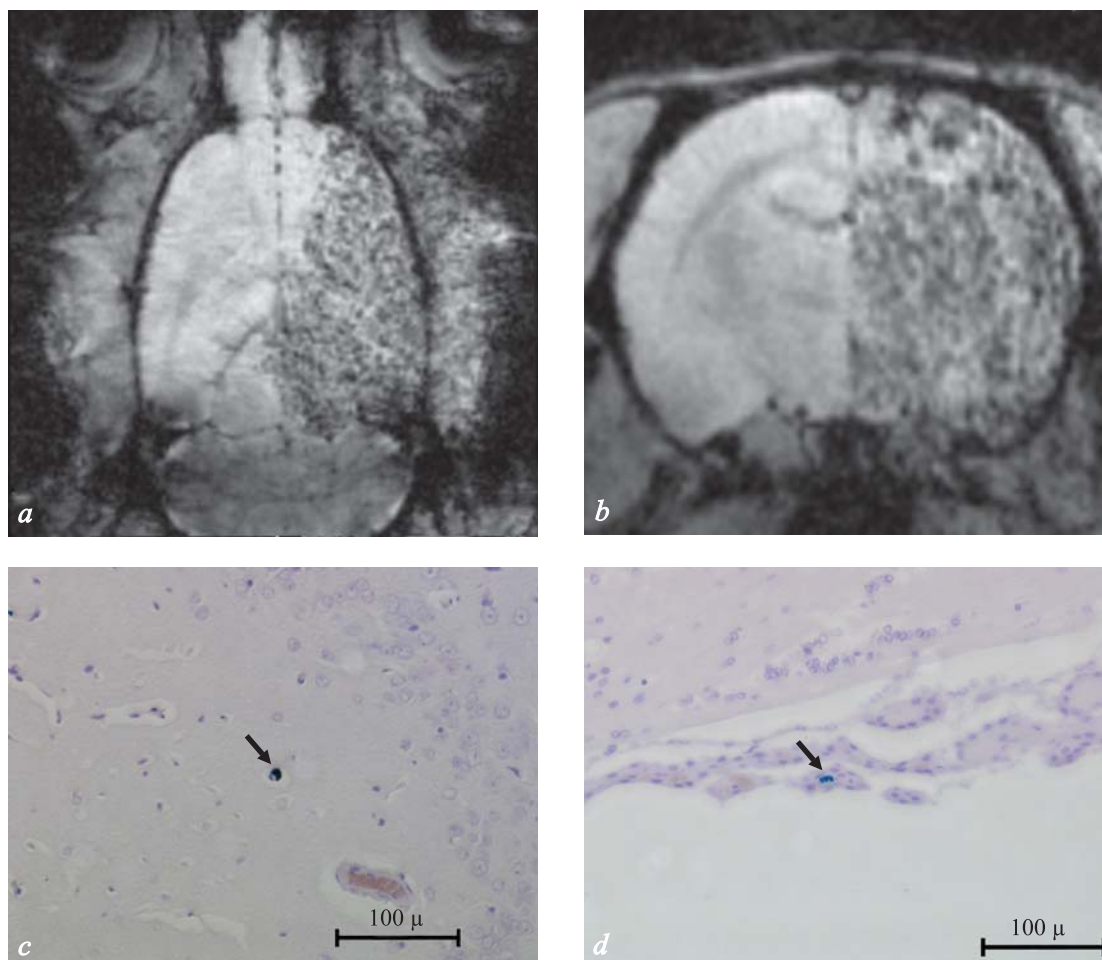


**Fig. 4.** Distribution of IOMP-labeled MMSC in the brain in 3 h after transplantation. Representative T2\*-weighed MRI sections of the brain in axial (a) and coronary (b) projections. Identification of IOMP-labeled MMSC on histological sections of the brain using Perl's staining. IOMP-labeled MMSC are shown by arrows.

is accumulated in the brain, while the greater part is distributed in the liver, kidneys, and bladder. In the course of biochemical transformations, the complex is gradually released from the brain and excreted by the liver and intestine. This distribution significantly differs from the distribution of  $^{99m}\text{Tc}$ -HMPAO-labeled cells.

On the model of brain injury, we have demonstrated more pronounced therapeutic effect of intraarterial transplantation of cells in comparison with their intravenous injection [14]. In this work, we have confirmed that intraarterial injection provides direct delivery of cells to the brain bypassing filtering organs, the lungs and the liver. Indeed, the number detected label in the liver and lungs was significantly lower after intraarterial injection of cells. These two facts suggest that the effectiveness of therapy depends on the number of cells in the focus of injury where the cells can secrete trophic and anti-inflammatory factors [7]. Possible blockage of small vessels with transplanted cells can also affect the distribution of cells in the body. The

role of the first capillary filter after intravenous injection is played by the lungs, and after intraarterial injection by brain vessels.

It should be noted that despite some studies of MMSC localization in various brain pathologies, our work is largely a pioneer study. Most studies on the cell therapy of brain pathologies are focused on the distribution of transplanted cells in the target organ, while non-target organs receive little attention, probably because of complexity of the majority of the used technologies (immunohistochemistry, histology, and fluorescent labeling), which makes difficult thorough examination of many organs, not to mention that most of these studies are possible only postmortem. It is well-known that reciprocal relationships between the organs can significantly modulate the course of the disease. Hence, the presence of transplanted stem cells in some other organs, in addition to the brain, theoretically can affect the course of neurological disease. Thus, some neuroprotective effects of transplanted stem cells in the therapy of cerebral ischemia can be

associated with their interaction with extracranial organs [3]. In this context, the dynamics of transplanted cells in vital organs should be carefully analyzed and the use of radioisotope labeling for cell identification opens new possibilities in this field.

Our study showed that visualization of  $^{99m}\text{Tc}$ -HMPAO-labeled stem cells by radionuclide scintigraphy is an objective and highly informative method allowing real-time *in vivo* tracing of cell distribution in the body.

The study was supported by the Russian Science Foundation (grant No. 14-15-00107).

## REFERENCES

- Barbosa da Fonseca LM, Gutflen B, Rosado de Castro PH, Battistella V, Goldenberg RC, Kasai-Brunswick T, Chagas CL, Wajnberg E, Maiolino A, Salles Xavier S, Andre C, Mendez-Otero R, de Freitas GR. Migration and homing of bone-marrow mononuclear cells in chronic ischemic stroke after intra-arterial injection. *Exp. Neurol.* 2010;221(1):122-128.
- Becerra P, Valdés Vázquez MA, Dudhia J, Fiske-Jackson AR, Neves F, Hartman NG, Smith RK. Distribution of injected technetium(99m)-labeled mesenchymal stem cells in horses with naturally occurring tendinopathy. *J. Orthop. Res.* 2013;31(7):1096-1102.
- Borlongan CV, Hadman M, Sanberg CD, Sanberg PR. Central nervous system entry of peripherally injected umbilical cord blood cells is not required for neuroprotection in stroke. *Stroke.* 2004;35(10):2385-2389.
- Chua JY, Pendharkar AV, Wang N, Choi R, Andres RH, Gaeta X, Zhang J, Moseley ME, Guzman R. Intra-arterial injection of neural stem cells using a microneedle technique does not cause microembolic strokes. *J. Cereb. Blood Flow Metab.* 2011;31(5):1263-1271.
- de Vries EF, Roca M, Jamar F, Israel O, Signore A. Guidelines for the labelling of leucocytes with (99m)Tc-HMPAO. Inflammation/Infection Taskgroup of the European Association of Nuclear Medicine. *Eur. J. Nucl. Med. Mol. Imaging.* 2010;37(4):842-848.
- Detante O, Moisan A, Dimastromatteo J, Richard MJ, Riou L, Grillon E, Barbier E, Desruet MD, De Fraipont F, Segebarth C, Jaillard A, Hommel M, Ghezzi C, Remy C. Intravenous administration of  $^{99m}\text{Tc}$ -HMPAO-labeled human mesenchymal stem cells after stroke: *in vivo* imaging and biodistribution. *Cell Transplant.* 2009;18(12):1369-79.
- Dihné M, Hartung HP, Seitz RJ. Restoring neuronal function after stroke by cell replacement: anatomic and functional considerations. *Stroke.* 2011;42(8):2342-2350.
- Feeney DM, Boyeson MG, Linn RT, Murray HM, Dail WG. Responses to cortical injury: I. Methodology and local effects of contusions in the rat. *Brain Res.* 1981;211(1):67-77.
- Frangioni JV, Hajjar RJ. *In vivo* tracking of stem cells for clinical trials in cardiovascular disease. *Circulation.* 2004;110(21):3378-3383.
- Hughes DK. Nuclear medicine and infection detection: the relative effectiveness of imaging with  $^{111}\text{In}$ -oxine-,  $^{99m}\text{Tc}$ -HMPAO-, and  $^{99m}\text{Tc}$ -stannous fluoride colloid-labeled leukocytes and with  $^{67}\text{Ga}$ -citrate. *J. Nucl. Med. Technol.* 2003;31(4):196-201; quiz 203-4.
- Nakamura K, Tukatani Y, Kubo A, Hashimoto S, Terayama Y, Amano T, Goto F. The behavior of  $^{99m}\text{Tc}$ -hexamethylpropyleneamineoxime ( $^{99m}\text{Tc}$ -HMPAO) in blood and brain. *Eur. J. Nucl. Med.* 1989;15(2):100-107.
- Plotnikov EY, Pul'kova NV, Silachev DN, Manskikh VN, Khryapenkova TG, Zorov DB, Sukhikh G.T. Methods of detection of mesenchymal stem cells in the kidneys during therapy of experimental renal pathologies. *Bull. Exp. Biol. Med.* 2012;154(1):145-151.
- Ratliffe E, Glen KE, Naing MW, Williams DJ. Current status and perspectives on stem cell-based therapies undergoing clinical trials for regenerative medicine: case studies. *Br. Med. Bull.* 2013;108:73-94.
- Silachev DN, Plotnikov EY, Babenko VA, Danilina TI, Zorov LD, Pevzner IB, Zorov DB, Sukhikh G.T. Intra-arterial administration of multipotent mesenchymal stromal cells promotes functional recovery of the brain after traumatic brain injury. *Bull. Exp. Biol. Med.* 2015;159(4):528-533.
- Viglietti AL, Perlo G, Augeri C, Massara C, Zaccaria S, Uccelli L, Boschi A. Radiochemical purity and stability of  $^{99m}\text{Tc}$ -HMPAO preparations: the influence of pH, volume recovery, and storage conditions. *Healthc. Prof. J.* 1(1-4):47-51.
- Zolle I. *Technetium-99m Radiopharmaceuticals. Preparation and Quality Control in Nuclear Medicine.* Berlin, 2007. P. 251-257.